Journal of Process Control 27 (2015) 38–49

Contents lists available at ScienceDirect

Journal of Process Control

journal homepage: www.elsevier.com/locate/jprocont

Control of self-assembly in micro- and nano-scale systems

Joel A. Paulson, Ali Mesbah, Xiaoxiang Zhu, Mark C. Molaro, Richard D. Braatz *

Department of Chemical Engineering, Massachusetts Institute of Technology, Cambridge, MA, USA

ARTICLE INFO

Article history:
Received 1 May 2014
Received in revised form 10 October 2014
Accepted 13 October 2014
Available online 17 December 2014

Keywords:
Self-assembly
Active self-assembly
Directed self-assembly
Controlled self-assembly
Nanotechnology
Systems nanotechnology
Microsystems
Microchemical systems

ABSTRACT

Control of self-assembling systems at the micro- and nano-scale provides new opportunities for the engineering of novel materials in a bottom-up fashion. These systems have several challenges associated with control including high-dimensional and stochastic nonlinear dynamics, limited sensors for real-time measurements, limited actuation for control, and kinetic trapping of the system in undesirable configurations. Three main strategies for addressing these challenges are described, which include particle design (active self-assembly), open-loop control, and closed-loop (feedback) control. The strategies are illustrated using a variety of examples such as the design of patchy and Janus particles, the toggling of magnetic fields to induce the crystallization of paramagnetic colloids, and high-throughput crystallization of organic compounds in nanoliter droplets. An outlook of the future research directions and the necessary technological advancements for control of micro- and nano-scale self-assembly is provided.

1. Introduction

Self-assembly is a process in which particles spontaneously arrange into complex patterns or organized superstructures [1]. Systems with self-organizing characteristics are commonly encountered in nature and engineered technologies, where particles can be of all scales ranging from molecules in a crystal to cells in a tissue to planets in a galaxy [2]. Bottom-up engineering of self-assembly systems enables manufacturing materials and devices with novel optical, mechanical, and electronic properties. The innovative applications of self-assembly at the micro- and nano-scales have sparked interest in understanding the physics, dynamics, and implementation of self-organizing systems. Control of self-assembly processes is key to the manufacture of materials with unique properties.

This paper aims to provide an overview on the recent progress of controlling self-assembly of micro- and nano-scale systems. Controlled self-assembly implies promoting or accelerating the organization of particles towards desired structures. Intervention is expected in a self-organizing process, for example, by changing the particle interactions [3,4] or by manipulating the environment (i.e., global system variables) in which self-assembly takes place [5–7]. This idea is often called "directed self-assembly" [8,9]. The concept should be distinguished from "directed assembly", which refers to the precise manipulation of particles one-by-one during the construction of the structure (like a mason building a brick wall) [5]. Directed assembly at the microscale is now considered standard manufacturing technology such as in three-dimensional printing (see e.g., [10–12] and the citations therein). In addition, directed assembly was recently demonstrated at the nanoscale by moving particles using the tip of an atomic force microscope [13,14]. Directed assembly has a very strong bottleneck from a manufacturing point of view due to the limiting speeds at which you can manipulate the building blocks of the system. For example, a reasonable estimate for the printing speed of a three-dimensional printer with resolutions on the micro- to macro-scale is $\sim$1 cm/s [15]. Assuming nanometer resolution is attainable with this printing speed, it would take $\sim 10^{14}$ s to print a device of 1 cm^3 volume with nanometer precision. Although directed assembly is a very active area of research, the topic is beyond the scope of this paper.

In the attempt to control self-assembly systems, many practical difficulties arise that are associated with the small-scale characteristics of the systems, which limit current technology and practice. This article outlines the major challenges in the control of self-assembly systems. Promising research directions in the areas of active self-assembly, open-loop control, and closed-loop control are motivated using examples from the literature. The paper concludes with perspectives on the research outlook of control of self-assembly systems.

* Corresponding author. Tel.: +1 617 253 3112; fax: +1 617 258 0542.
E-mail address: braatz@mit.edu (R.D. Braatz).

http://dx.doi.org/10.1016/j.jprocont.2014.10.005
0959-1524/

2. Challenges

2.1. High-dimensional stochastic nonlinear dynamics

In macroscopic systems, measured variables (i.e., outputs) typically are stochastic due to sensor noise and unknown disturbances arising from environmental fluctuations in variables (e.g., temperature) acting on the system. Isolated stochastic terms can be included in deterministic models to account for this behavior on the macroscale [16]. In other words, the measured outputs of macroscale systems are most often deterministic in the absence of noise and unknown disturbances.

Micro- and nano-scale systems are different in that their underlying phenomena are *inherently stochastic* so that repeated experiments can produce different results even if the system has no noise or unknown disturbances [17]. This inherent stochasticity can greatly impact the self-assembly of particles at these scales. For example, self-assembly of colloidal particles (at fixed conditions) can require excessively long periods of waiting time before initiation of the first step of the process (e.g., nucleation) needed to make a product, due to the first step having a high-energy activation barrier [5]. Another example is a microfluidic platform that uses evaporation to induce crystal nucleation of organic compounds such as amino acids and proteins [18,19]. The measured output for a single droplet is the *induction time* (i.e., the time at which the first crystal nucleates) and is best represented as an induction time *distribution* due to the stochastic nature of the system.

Stochastic dynamics with continuous states are typically described by Langevin equations [20–22], which describe the time evolution of a group of variables that change slowly relative to other variables in the system. The original Langevin equation was derived as a modification to Newton's equations of motion to include Brownian motion and frictional drag due to collisions of particles (slow variables) with the solvent (fast variables). This system can be formulated as a stochastic differential equation (SDE) of the form [23]

$$d\mathbf{X}_t = \boldsymbol{\mu}(\mathbf{X}_t, t)dt + \boldsymbol{\sigma}(\mathbf{X}_t, t)d\mathbf{W}_t, \tag{1}$$

where $\mathbf{X}_t \in \mathbb{R}^n$ denotes an n-dimensional stochastic process, $\boldsymbol{\mu} = (\mu_1, \ldots, \mu_n)$ denotes the drift vector, $\mathbf{W}_t$ denotes an m-dimensional Weiner process (i.e., Brownian motion), and $\boldsymbol{\sigma} = [\sigma_{ij}]$ is directly related to the diffusion tensor $\mathbf{D} = [D_{ij}]$ with elements

$$D_{ij}(\mathbf{X}_t, t) = \frac{1}{2}\sum_{k=1}^{m}\sigma_{ik}(\mathbf{X}_t, t)\sigma_{jk}(\mathbf{X}_t, t). \tag{2}$$

This SDE is nonlinear and difficult to solve directly. Methods such as Monte Carlo simulation or Molecular Dynamics (MD) are available for obtaining time-averaged quantities of interest while avoiding direct simulation of (1). However, these methods are very computationally expensive and are only able to simulate complex systems for a very short period of time.

The dynamics of self-assembling systems involve the evolution of hierarchical components at different time scales due to their architecture (e.g., atoms make up proteins, proteins make up capsomers, and capsomers make up viral capsids [24]). Eq. (1) alone cannot describe this behavior; instead, a multiscale approach is required (e.g., see [25]). However, multi-scale modeling approaches are very computationally expensive, taking on the order of days to simulate a relatively small self-assembly system (a system consisting of ~50 particles) using standard personal computers.

For systems with a discrete number of possible states, the stochastic dynamics are described by the Master equation [26,27]

$$\frac{dP_\sigma}{dt} = \sum_{\sigma'} w_{\sigma'\to\sigma}(t)P_{\sigma'}(t) - \sum_{\sigma'} w_{\sigma\to\sigma'}(t)P_\sigma(t), \tag{3}$$

where $P_\sigma(t)$ denotes the probability that the system is in configuration σ at time t and $w_{\sigma'\to\sigma}(t)$ denotes the rate of transition from configuration σ' to configuration σ at t. The overall system is described by writing (3) (i.e., conservation equation for probability of configuration σ) for every possible configuration of the system. The probabilities can be stacked into a state vector $x(t)$ and the transition rates collected into a matrix $A(t, u(t); p)$ so that (3) can be written in the state-space form

$$\frac{dx}{dt} = A(t, u(t); p)x(t), \tag{4}$$

where $A(t, u(t); p)$ depends on time-varying variables (e.g., temperature), system inputs (i.e., manipulated variables) $u(t)$, and model parameters p such as chemical kinetic rate constants, diffusion coefficients, and thermodynamic properties of the system.

The main challenge in implementing control systems for processes modeled by (4) is that the number of states is usually very large (usually much greater than 10^{10}) for processes of practical importance [17]. Kinetic Monte Carlo (KMC) simulations are commonly used to approximate the solution of (4) by computing specific realizations of the Master equation. This approach uses calls from a random number generator to select a specific event to occur from a queue of all possible events, along with its corresponding time step, so that the time simulated in the KMC algorithm corresponds to real time [26]. Although this approach is usually much faster than solving (4) directly, KMC simulations can still take in the order of days for realistic systems. If state or output distributions are required for control, then a large number of KMC simulations are needed, which makes real-time control infeasible even for relatively simple systems. If the control objective depends only on coarse statistics of the distribution, then one approach is to develop low-order "equation free" models (e.g., [28,29]) by fitting the KMC simulation results; however, the relationship between the manipulated variables and the system states in these models will no longer be transparent, making control less intuitive and more black box in nature [17].

2.2. Limited sensors for real-time measurements

Controlling self-assembly systems at the micro- and nano-scale requires the acquisition of real-time information about the system status. This requirement leads to the needs of advanced real-time sensing techniques, while traditional self-assembly systems often rely on imaging or other characterization techniques performed after the assembly process to measure the local properties (e.g., using transmission electron micrographs to inspect the morphology in a self-assembling block copolymer system [30]).

Several factors result in real-time sensing in self-assembly systems being a challenge, including the small length scales, the slow and invasive nature of most observation techniques, and the limited variables that can be used to quantify the system status. For crystallization in a nanoliter droplet implemented in a microfluidic platform [18,19,31], the small scale of the system inhibits implementing conventional methods of probing the solute concentration. While visual observation of the dynamics in self-assembled systems could be accessible through advanced microscopes (such as the fluorescent imaging technique used to track the real-time movement and clustering of Janus particles [32]), such information has to be translated into a variable that can represent the assembly status for control.

2.3. Limited actuation for control

Another challenge that naturally arises in controlling self-assembly systems is the limited availability of actuators. For a micro- or nano-scale self-assembly system, localized manipulation

by *local actuators* to influence the assembly of the particles is constrained. Instead, controlling the self-assembly process typically relies on manipulating macroscopic variables in the system (denoted *global actuators*). The underlying principle is that changing the global properties can change the dynamic pathways of assembly. For example, during crystallization, optimized temperature control can improve the yield of one particular crystal polymorph over another [33,34]. The number of such global variables that can be useful for altering the state of assembly are somewhat limited, which often includes temperature, pressure, concentration, composition, and, for some systems, external fields such as electric and magnetic fields.

The use of the macroscopic variables as actuators acting globally on the system implies an impact on all particles—no matter what the particle association state is. This non-specific action may lead to disruption of already formed structures. On the other hand, identifying the relationship between actuation and system response, as well as specifying the amount of actuation in order to drive the system towards the desired state of assembly, is not trivial. The task may become even more challenging when a system has complicated dependency on the variables used as the actuators. For example, the formation of snowflakes from water vapor is very sensitive to the particular changes in temperature and pressure [35].

2.4. Kinetic traps in the energy landscape

Self-assembling systems typically have a range of stable or metastable configurations that can have vastly different structures and properties [36,37]. A common but practically important example of multiple configurations is crystal polymorphism, which is the ability of a compound to crystallize as one or more distinct crystal species. Different polymorphs of a compound have different molecular structures and usually very different properties such as solubility, melting point, density, hardness, vapor pressure, optical properties, and electronic properties [38].

Although most self-assembling systems have one lowest energy state (i.e., the state that is thermodynamically favored), systems can become trapped in "kinetically arrested" states associated with local minima in the free energy landscape, giving rise to various metastable configurations (e.g., glasses, gels, polycrystals) [5]. For example, suspensions of micrometer-sized paramagnetic colloidal spheres form disordered entangled chain-like structures in a steady magnetic field at high field strengths, where thermodynamic calculations indicate that the formation of well-ordered crystallization domains is favored. The thermodynamically most stable crystalline state is not observed experimentally because the system is trapped in the entangled state and the energy barrier is too high for the system to overcome in a reasonable amount of time [7]. Avoiding kinetically arrested states is key to consistently achieving the thermodynamically most stable state and is an important issue to account for when designing control laws for self-assembling systems.

3. Promising research directions

This section describes some promising approaches for addressing the aforementioned challenges (see Section 2) in the control of micro- and nano-scale self-assembly systems. These approaches can be grouped into three broad categories: active self-assembly (particle design), open-loop control, and closed-loop control. The advantages and disadvantages of these different approaches are illustrated through the use of examples.

Sufficiently general systems engineering methods for multiscale systems can be applied to self-assembly systems, which have been discussed in detail in past reviews (e.g., see [17,39,40] and the citations therein). These methods are well-known and will not be discussed in this paper, mainly because multiscale system techniques applied to small-scale self-assembling systems are computationally expensive and do not take advantage of underlying structure that can facilitate control tasks such as parameter estimation and feedback control [17].

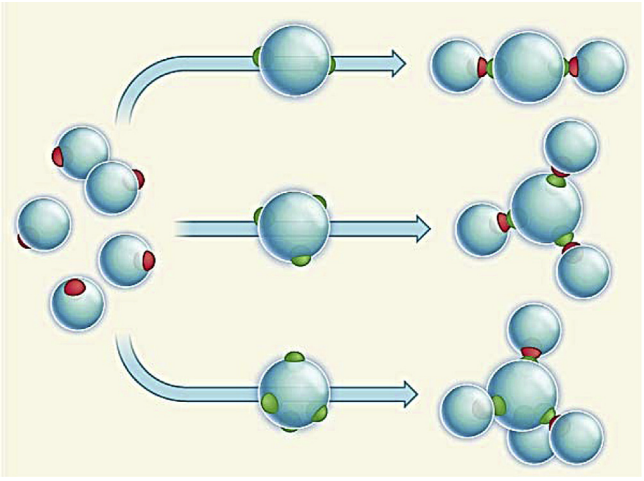

Fig. 1. Active self-assembly of patchy particles enables bottom-up construction of sophisticated structures from smaller particles. Red and green regions are surface patches positioned on particles to govern directional interactions between particles and particle specificity. The surface patches resemble the arrangements of bonds around atoms. Reprinted by permission from Macmillan Publishers Ltd: Nature [4], Copyright 2012. (For interpretation of the references to color in this figure legend, the reader is referred to the web version of this article.)

3.1. Active self-assembly

In active self-assembly [41–43], particles interact to reach a *consensus* regarding the desired global behavior of a self-organizing system, which depends on the state of all particles. The interactions among the particles are governed by a *consensus protocol* that specifies the information exchange between a particle and all of its surrounding particles. The primary challenge in active self-assembly is how to task the individual particles so that the global behavior of a self-organizing system is engineered (e.g., a desired structure emerges) with high probability, despite the stochastic nature of the system. This tasking requires the ability to design *local rules* for individual particles, which ensure the unique convergence to a pre-specified global behavior with the fastest convergence rate [42].

Active self-assembly provides opportunities for *bottom-up engineering* of micro- and nano-scale systems such as proteins in cells and nanoscale molecular machines. Self-assembly of *patchy particles* [4] has emerged as an effective approach to actively control structures that are assembled from small particles. Placing sticky patches on particles can cause the particles to interact only along certain directions and, therefore, alleviates the lack of specificity of particles (see Fig. 1). Generation of directional interactions between patchy particles mimics atomic bonding in molecules, and can significantly increase the structural complexity of a self-organizing system (see e.g., [44,45] and the citations therein for detailed discussions on patchy particles/colloids and how their self-assembled patterns can be theoretically predicted). For example, Wang et al. [46] synthesized micrometer-sized particles with symmetrically arranged sticky patches of DNA on their surfaces to enable DNA-mediated interactions. The single-stranded DNA molecules attached to the patches mediate interparticle binding through hybridization with complementary DNA strands attached

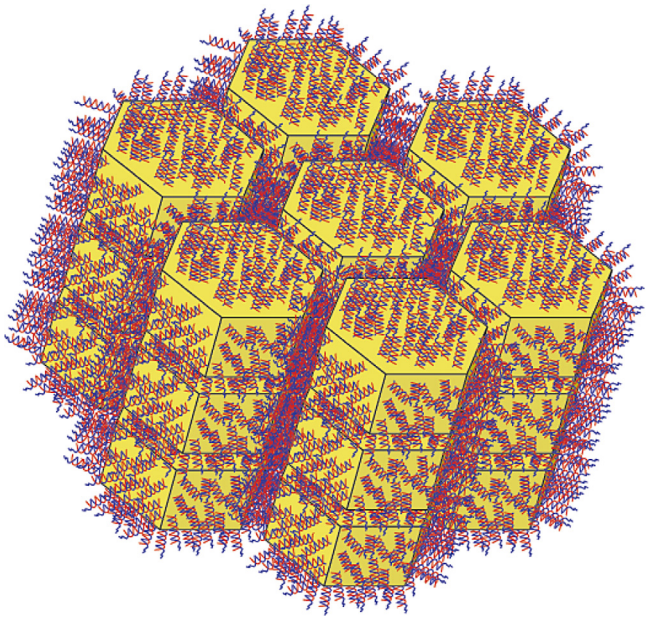

Fig. 2. A schematic of a hypothetical system of hexagonal prisms assembled from DNA-functionalized nanoparticles, which represents a type of active self-assembly. Double-stranded DNA is attached to the gold nanoparticles on the surface. A small strand of self-complementary single-stranded DNA acts as a sticky patch at the end of the DNA linker to which the DNA on other nanoparticles is attached. Reprinted by permission from Macmillan Publishers Ltd: Nature Materials [3], Copyright 2010.

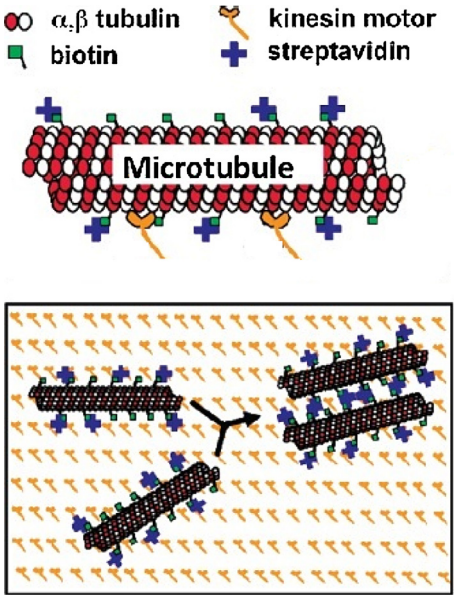

Fig. 3. Active self-assembly of millimeter-scale wires using nano-scale transport. Surface-adhered kinesin motor proteins enable transport of biotinylated microtubules, which form microtubule bundles due to cross-linkage of streptavidin. Reprinted (adapted) with permission from [47]. Copyright 2011 American Chemical Society.

to patches on neighboring patches. In such a particle, the location of patches governs the directionality, and the sequence-dependent binding of DNA dictates specificity.

Patchy particles have been used to synthesize artificial molecules by combining mixtures of particles that have matched directional interactions and complementary DNA strands, such as DNA-functionalized gold nanoparticles shown in Fig. 2 [3]. In addition, an energy source can be used to accelerate the movement of particles, while modifying the particle interactions using sticky patches. Fig. 3 shows the assembly of biotinylated microtubules partially coated with streptavidin into linear bundles [47]. The movement of the biotinylated microtubules is facilitated by gliding them on a surface coated with kinesin motor proteins, which can result in gliding velocities up to 1 μm/s. The streptavidin coating enables microtubules to cross-link into microtubule bundles.

Similarly, *Janus particles* that combine incompatible elements in the same unit structure lead to the formation of persistent and defect-free superstructures [48]. This *ambivalence principle* is ubiquitously used in nature to create complex self-organizing structures. Examples are the formation of biological membranes from self-assembly of phospholipid molecules with polar head groups and hydrophobic tails, or the formation of a DNA strand from nucleotides that consist of a part capable of forming hydrogen bonds and an inert part. Applications of Janus particles are emerging for bottom-up manufacturing of complex matter through spontaneous self-assembly. It has been shown that, when immersed in an aqueous salt solution, spherical Janus particles (e.g., symmetric micelle structures) that are hydrophobic on one hemisphere and polar on the other polymerize into elongated strings and branched anisotropic structures [49].

3.2. Open-loop control

Any reader of this journal knows the use of the term *open-loop control* to describe a system whose input profiles are set *a priori* (not informed by measurements/feedback). Open-loop input profiles can be computed heuristically, based on experimental observations and intuition, or using a model-based optimization, which requires a mathematical formulation of the system and control objective. For complex systems, a hybrid approach can be used to embed heuristic knowledge of the system in the optimization procedure and, therefore, reduce the complexity of the problem.

Open-loop control strategies are independent of measurements, which is the only option for micro- and nano-scale self-assembling systems that do not have real-time sensors available (see Section 2.2). However, the reduced information comes at the expense of robustness (i.e., the ability of the controller to reject disturbances, model imperfections, etc. by accounting for the current measured system state). The impact of feedback control using real-time measurements is explored in Section 3.3. As discussed in Section 2.3, actuators that drive micro- and nano-scale self-assembly can be introduced either globally (changes felt throughout the system) or locally (changes felt only in the local environment). Global actuators act on the macroscopic scale where it is easier to implement the manipulation, but do not provide the controllability enabled by local manipulations. Local actuators are more challenging to implement experimentally, but enable more effective actuation at the micro- and nano-scale.

A recent example of an open-loop control procedure developed *heuristically* using a single *global actuator* is the self-assembly of paramagnetic colloids into well-ordered crystalline domains using toggled magnetic fields [7]. The experimental setup is shown in Fig. 4. When no magnetic field is applied, the colloidal suspension remains dispersed in solution. In a constant magnetic field, the colloidal suspension forms chains parallel to the magnetic field lines, which start to aggregate laterally. The aggregation arrests the motion of the particles and leaves them in an entangled/disordered state that is at higher energy than the thermodynamically favored state of well-ordered crystalline domains.

Toggling the magnetic field on and off at particular frequencies enables the suspension as a whole to quickly enter its lowest energy state (well-ordered crystals). This open-loop control strategy is effective because, when the magnetic field is turned off, the attractive interactions between the colloids are suppressed

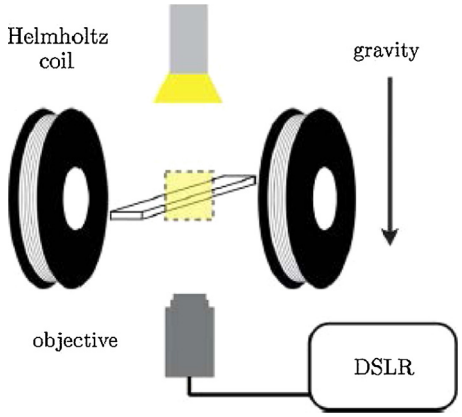

Fig. 4. Illustration of the experimental apparatus used to drive the assembly of paramagnetic colloids via toggling the external magnetic field. A pair of Helmholtz coils are used to generate the magnetic field (whose field lines are normal to the gravitational field) and a DSLR camera was used to generate images. The suspension is deposited on a glass slide with a coverslip so that the colloids can only move in the horizontal plane perpendicular to gravity due to their strong sedimentation. Reproduced from [7] with permission from The Royal Society of Chemistry.

allowing the particles to relax and reconfigure (thus breaking out of the kinetically trapped state) and reach the desired state in a much shorter period of time. In a constant magnetic field, the entangled chains are unlikely to break apart due to the attractive forces between the colloids, which creates a high energy barrier that traps the suspension in this disordered state.

The toggling frequency is the key parameter in such systems since the time that the field remains off must be long enough for the suspension structure to rearrange but not long enough for the colloids to diffuse very far and redisperse. That is, the toggling frequency should be similar to the characteristic relaxation rate of the suspension. The time evolution of the suspension at different toggling frequencies measured in [7] is shown in Fig. 5, where the dark regions represent the particle-rich phase. All frequencies form the entangled/disordered (unfavorable) state initially. As time increases, the chains start to merge and the system begin to "coarsen." The near-optimal toggling frequency is ~0.5–1 Hz, where the coarse chains start to break apart at ~500 s and form the desired state of well-ordered crystals (the favored state) after ~2000 s.

The open-loop approach of cycling manipulated variables has proved useful in a variety of self-assembly processes, where the particles in the system are indistinguishable. Another related example is the use of temperature cycling in crystallization to change crystal shape, enhance crystal size uniformity, and increase polymorphic purity [50,51].

An interesting alternative to these methods, which can increase precision/controllability in small-scale self-assembling systems, is to introduce small external controls (e.g., electric charges, magnets). The external controls introduce attractive or repulsive interactions to the system potential energy to drive the system towards a particular configuration. Two approaches have been proposed for the design of these external controls:

1. Robust Static Structures – What are the optimal external controls (number/locations/strengths) so that the self-assembled micro- or nano-structure is stable to a desired degree of robustness (i.e., obtained with a sufficiently high probability in spite of system stochasticity)?
2. Robust Dynamic Paths – What external control profiles over time are needed to ensure that, with a high probability, the system evolves to the desired structure from any initial distribution of particles?

The theoretical challenges associated with these systems-level questions are explored in detail in a two-part series (Robust Static Structures in [52] and Robust Dynamic Paths in [53]). This work falls into the open-loop control category of optimal *local actuation* computed using *model-based optimization*.

Algorithms for computing energy landscapes such that the system remains in the desired configuration with a sufficiently high probability are proposed in [52] (please refer to [52] for a detailed discussion of these algorithms and their results as they are only summarized here). An energy functional is proposed of the form [52]

$$E(\mathbf{z}) = \underbrace{\sum_{i=1}^{V}\sum_{k=1}^{N_d} z_i H_{i,k} s_k}_{E_{\text{ext}}(\mathbf{z})} + \underbrace{\sum_{i<j} z_i J_{ij} z_j}_{E_{\text{int}}(\mathbf{z})} = \mathbf{z}^{\mathrm{T}}\mathbf{H}\mathbf{s} + \mathbf{z}^{\mathrm{T}}\mathbf{J}\mathbf{z}, \tag{5}$$

where $\mathbf{z} \in \{0, 1\}^V$ denotes the system configuration with $z_i = 0$ indicating an empty lattice site and $z_i = 1$ indicating the presence of a particle, V denotes the system volume (i.e., number of available lattice sites), N_d denotes the number of external field controls, $\mathbf{s} \in \mathbb{R}^{N_d}$ denotes the configuration of the external field controls with s_k being the strength of the kth external field, $H_{i,k}$ denotes the interaction between the ith lattice site and the kth external field, J_{ij} denotes the interaction between the ith and jth lattice sites, and the superscript T refers to the vector transpose. The first sum $E_{\text{ext}}(\mathbf{z})$ represents the external field's contribution to the system energy while the second sum $E_{\text{int}}(\mathbf{z})$ represents the interactions between particles in the system. Higher-order interaction terms can easily be incorporated into this model if necessary (depending on the underlying physics of the system).

The first step of the static problem [52] is to *qualitatively* shape the energy landscape by determining the number N_d and locations of the required well- and barrier-forming point conditions (external controls) to keep the desired self-assembled structure in place (termed the *minimum tiling problem*). The goal of the minimum tiling problem is to reduce the number of degrees of freedom in the system to be practical both from an implementation and optimization point of view. Given the number N_d and locations of the point-conditions, the second step is to *quantitatively* shape the energy landscape by determining the strengths of these point conditions to maximize the probability of the desired configuration, i.e.,

$$\max_{\mathbf{s}\in\mathbf{S}} p(\mathbf{z}_d, \mathbf{s}) = \max_{\mathbf{s}\in\mathbf{S}} \frac{e^{-\beta E(\mathbf{z}_d,\mathbf{s})}}{\sum_{\mathbf{z}_j \in \Omega_\alpha} e^{-\beta E(\mathbf{z}_j,\mathbf{s})}}, \tag{6}$$

where $p(\mathbf{z}_d, \mathbf{s})$ denotes the probability of desired state $\mathbf{z}_d$ given external control field $\mathbf{s}$, and $\mathbf{S}$ denotes the set of all possible point condition strength values. The canonical Boltzmann probability distribution function (constant particle number, volume, and temperature) is used here to calculate $p(\mathbf{z}_d, \mathbf{s})$ based on the energy function (5). The parameter β determines the "flow" of system through the system phase space (low β implies more accessibility of the states to the system). The denominator represents the *partition function* and is defined as a sum over all configurations Ω_α (see [54] for a detailed discussion on the use of partition functions in the quantitative prediction of self-assembly). Numerous ways to solve this problem are discussed in detail in [52] and the resulting optimal control policy $\mathbf{s}^*$ is applied once the system reaches the desired configuration.

To dynamically force the system to this desired configuration, a method was developed that progressively restricts the system phase space (i.e., allowable configurations) to smaller and smaller regions of the physical domain (see Fig. 6) [53]. The basic idea

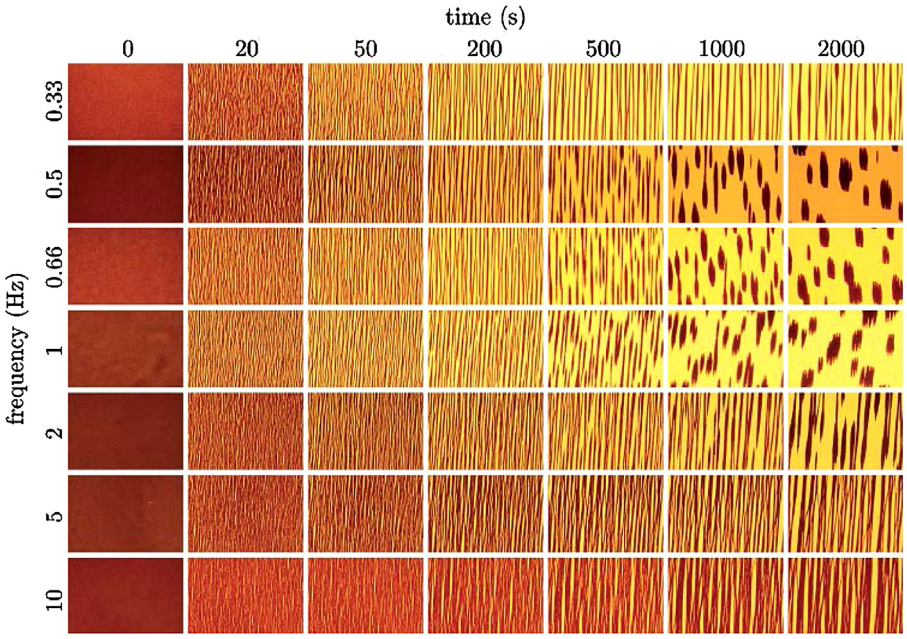

Fig. 5. The time evolution of a suspension of paramagnetic colloid particles (dispersed in ultra-pure water with a volume fraction of 0.5%) under the influence of a toggled magnetic field that is turned on and off at various frequencies (denoted toggling frequency). The magnetic field strength is 1500 A/m. Each image is 3.2 mm × 2.1 mm in dimension. All suspensions appear to reach their final/slowly evolving state after ~2000 s. There is a clear region near 0.66 Hz in which the suspension condenses into large crystalline domains (favored state). At high toggling frequencies (≥5 Hz), the suspension remains trapped in the unfavorable entangled/disordered state. At 0.33 Hz, the kinetics of chain-breaking appear to slow significantly so that it will take a long time to reach the favored state of large crystalline domains. This represents an open-loop control policy for magnetic toggling frequency that was computed heuristically. Reproduced from [7] with permission from The Royal Society of Chemistry.

is to systematically break the phase space up into *components* (i.e., subsets of phase space in which all configurations in the subset are accessible from any other configuration in the same subset). This decomposition occurs during distinct time periods denoted as "stages" where the starting stage 0 comprises the entire phase space. At the end of each stage, the starting component will be decomposed into two subsets—one of which will be processed further and another that is neglected. Take, for example, a system described in [53] shown in Fig. 6b. Stage 0 shows that the 6 particles can be in any combination of the 16 lattice sites. During stage 1, the objective is to drive the system to have 5 particles in the left half of the domain and 1 particle in the right half of the domain. Although a number of configurations satisfy this requirement, the target configuration is restricted to be within a particular subset of phase space. During each stage, the system is further restricted until the desired configuration is reached in the final stage.

To achieve this progressive restriction of phase space, Solis et al. [53] proposed solving a series of pseudostatic optimization problems over time until the system reaches equilibrium, with the optimization at stage k being

$$\max_{\mathbf{s}^{(k)}\in\mathbf{S}} p(\Omega_\alpha^{(k)}, \mathbf{s}^{(k)}) = \max_{\mathbf{s}^{(k)}\in\mathbf{S}} \frac{\displaystyle\sum_{\mathbf{z}_j\in\Omega_\alpha^{(k)}} e^{-\beta E(\mathbf{z}_j,\mathbf{s}^{(k)})}}{\displaystyle\sum_{\mathbf{z}_j\in\Omega_\alpha^{(k-1)}} e^{-\beta E(\mathbf{z}_j,\mathbf{s}^{(k)})}}, \tag{7}$$

which is essentially maximizing the probability of the system moving into the restricted set of configurations $\Omega_\alpha^{(k)}$ from the set of configurations of the previous stage $\Omega_\alpha^{(k-1)}$ (as the domain is halved at each stage, the resolution of the $\Omega_\alpha^{(k)}$ is $1/2^k$). This optimization looks very similar to that of the static problem (6) and the same minimum tiling ideas can be used to determine the number and locations of the external controls $\mathbf{s}^{(k)}$ at each stage. This maximization is a nonlinear nonconvex optimization with a combinatorial number of potential configurations. A "genetic algorithm" is described in [53] for solving this complex problem; however, convergence and global optimality of the solution are not guaranteed.

The lack of measurements in the latter approaches implies that the (stochastic) system evolution is unknown since the positions of the particles are never observed. This no-measurements situation naturally gives rise to stochastic models for describing the system dynamics such as (1) and (3). In [55], a Master equation model was used in conjunction with the aforementioned methods of [52,53]. It is shown that open-loop control schemes can drive the self-assembly of the system (in simulations) to a targeted configuration with high probability. The main challenges for this task are estimating the parameters in the Master equation model and designing the physical actuators. These techniques provide a mathematical framework for controlling the self-assembly process and have the potential of constructing systems of higher complexity from simple particles than what is attainable by manipulating global field variables.

Strong specific interactions between particles can be used to achieve self-assembly of specifically tailored structures (see Section 3.1), however, these design strategies can result in kinetically trapped irregular/undesirable structures that are unable to reorganize on relevant time scales. The prevalence of specific interactions that are weak and reversible, on the other hand, allows dynamic reorganization that can enable systems to explore a wider range of geometric configurations thereby increasing the probability that the thermodynamically favored self-assembly structure will eventually form [56]. Moreover, certain particles have shown the ability to combine local specific order-determining interactions with delocalized non-specific interactions (attraction or repulsion) to achieve robust self-assembly.

Recently, this behavior was studied with the three-legged protein clathrin, which plays an important role in reshaping the cell membrane during endocytosis [56]. Self-assembly of

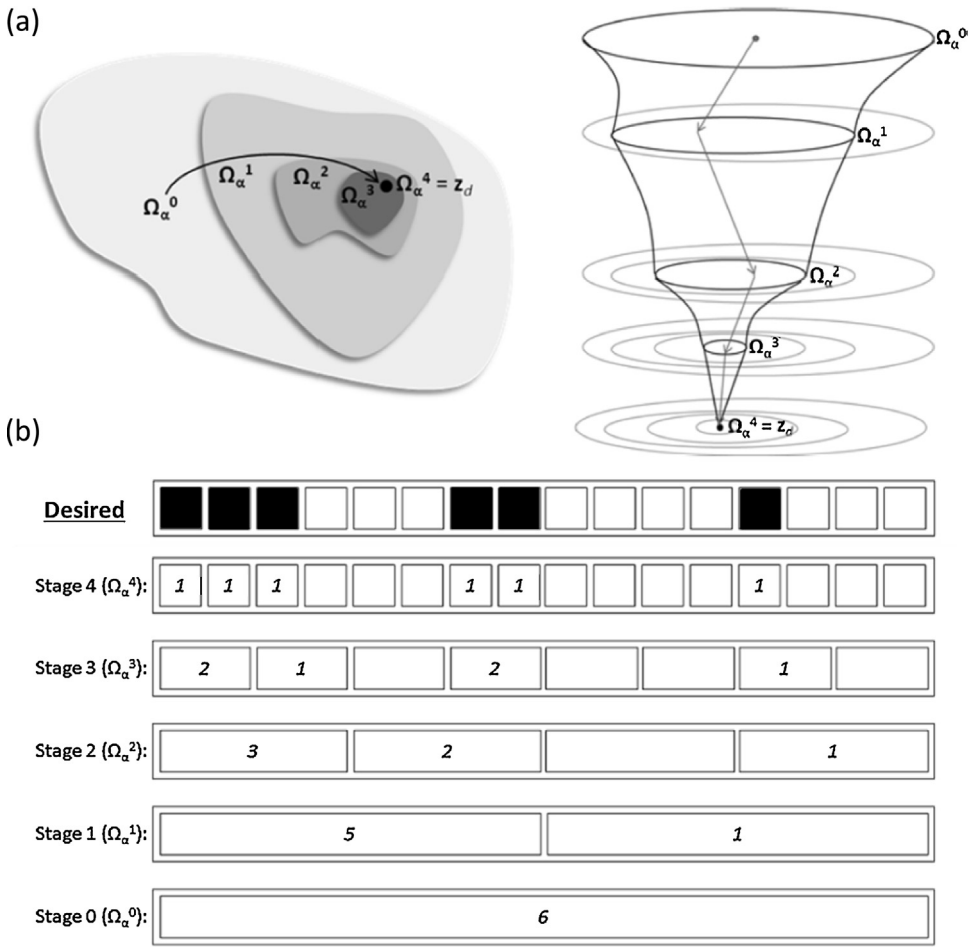

Fig. 6. Open-loop control policy used to drive the system to a desired arrangement of particles. Please refer to the text in Section 3.2 for detailed descriptions of this figure and the underlying optimization problems that must be solved to derive the control law. (a) Dynamic path that restricts the system to progressively smaller subsets of the system phase space (denoted Ω_α^i for the ith stage). (b) A one-dimensional example of the phase space restriction. Reprinted (adapted) with permission from [53]. Copyright 2010 American Chemical Society.

clathrin is stabilized by multiple (specific) weak leg–leg interactions [57]. Three main states were observed during clathrin assembly: monomer, assembled cages, and disordered aggregates. Experimental results from [56] indicate that two distinct kinetic routes occur in clathrin self-assembly. At pH values above the isoelectric point (IEP) of clathrin (pH = 5.8), the assembly proceeds monotonically from monomers to cage structures. At pH values below the IEP, the protein quickly forms disordered aggregates in solution that subsequently form cage structures over time due to large-scale remodelling of the clathrin aggregates. Cryo transmission electron microscopy images of clathrin assemblies at pH = 6.0 and pH = 5.1 from [56] clearly show these distinct paths (Fig. 7).

Both of these kinetic routes lead to similar final self-assembled states, which suggests that the mechanism of clathrin assembly has evolved to be robust. Brownian dynamics simulations suggest that stronger non-specific interactions in the system, which are likely caused by clathrin becoming increasingly hydrophobic at pH below the IEP, result in aggregation [56]. These results suggest that non-specific interactions, such as hydrophobic condensation due to local pH changes, can be used as additional degrees of freedom for robustly controlling self-assembly in an open-loop setting (without measurements), and that the use of multiple weak specific interactions can allow the system to escape disordered kinetically trapped states while still forming a desired ordered structure. These phenomena have been shown to be important in a number of other systems including, for example, the formation of a kagome lattice structure from colloids [8] and two-dimensional S-layer protein assembly on supported lipid bilayers [58].

3.3. Closed-loop control

In *closed-loop* control, system output measurements are used to compute the input profiles repeatedly based on the current state of the self-organizing system. Measurement feedback enables effective handling of system stochasticity, as the incorporation of measurements in the control input synthesis robustifies the inputs to uncertainties to a large extent. Such a control approach is capable of coping with the inherent stochastic nature of self-assembly, and facilitates driving the system towards a desired structure in the presence of uncertainties.

Feedback control techniques can improve performance compared to their open-loop counterparts. To illustrate this point, consider the nucleation of organic compounds (e.g., amino acids, proteins, and active pharmaceutical ingredients) within droplets of solution using a high-throughput microfluidic platform (see Fig. 8). The crystallization of crystals in small volumes requires the use of stochastic models (e.g., [31]). The nucleation and growth processes for the microfluidic platform in Fig. 8 can be modeled by a Master equation (3). When only the number of crystals is considered (i.e., nucleation events), the Master equation can be solved analytically as a function of time [31]. However, when the state is extended to include the length of all crystals (i.e., nucleation and growth), the

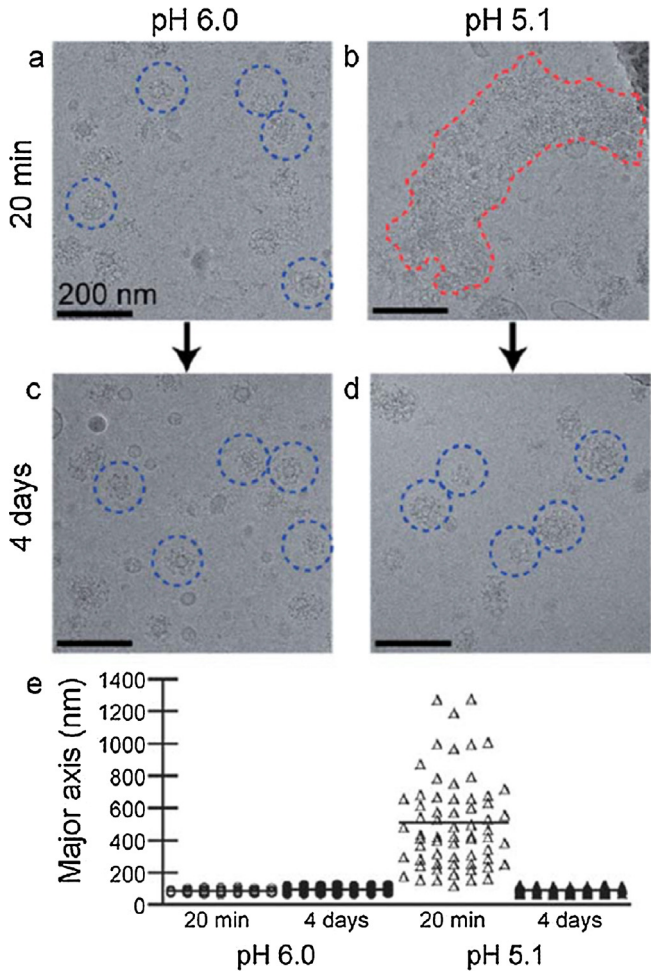

Fig. 7. Experimental demonstration that clathrin self-assembly is robust to changes in pH due to weak specific interactions. This methodology can be useful for designing open-loop control policies to be more robust. (a and c) Cryo transmission electron microscopy (TEM) image of clathrin self-assembly at pH = 6.0 after 20 min and 4 days. (b and d) Cryo TEM image of clathrin self-assembly at pH = 5.1 after 20 min and 4 days. Representative spherical cages and disordered aggregates of clathrin are outlined in blue and red, respectively. (e) Dot plot showing the major axis distribution of ellipses fit to the clathrin assemblies at pH = 6.0 (circles) and pH = 5.1 (triangles) after 20 min (open) and 4 days (filled). Solid lines represent the mean value (n = 63, 169, 64, and 54). Reproduced from [56] with permission from The Royal Society of Chemistry. (For interpretation of the references to color in this figure legend, the reader is referred to the web version of this article.)

number of Master equations becomes infeasible to construct/solve directly and a KMC strategy must be used to generate approximate statistical results from the model.

The input to this system is the volume of the droplet, which can be manipulated directly by changing the properties of a local reservoir that sets the evaporation rate (see [19]), and the output of interest is the number of crystals produced in the droplet. The rate expressions and parameter values used in all model simulations are given in [19,31] for lysozyme. For all simulations, the droplet initially has a total volume of 5 μL, a protein loading (C_{protein}) of 18 g/L, a salt concentration (C_{salt}) of 0.36 M, and a solubility curve defined by $C_{\text{protein-eq}} = 1.57C_{\text{salt}}^{2.94}$ g/L, where $C_{\text{protein-eq}}$ denotes the equilibrium (saturated) protein concentration.

The desired number of crystals at the final time was chosen to be 1 with a time horizon of 99 hr for all simulations. A proportional controller was used to determine the input applied to the system based on measurements. In the simulations, measurements of the number of crystals in the droplet were taken every 0.1 hr where the crystals could only be observed once they grew larger than 0.1 μm. Fig. 9 compares the distribution of the system output for closed- and open-loop operation. The open-loop input profile results in the formation of zero crystals approximately 30% of the time, which is extremely undesirable since that result produces no crystals for analysis and would require repeating the experiment. On the other hand, closed-loop control is able to compensate for stochastic fluctuations in the system (e.g., in the induction time) by altering the droplet volume in response to observing a crystal form, which results in the precipitation of at least one crystal in every simulation.

In another example, the use of feedback to control the self-assembly of silica colloids was recently demonstrated experimentally [5], with the configuration shown in Fig. 10A. The colloid positions are sensed in real time with an optical microscope (Fig. 10B) while the electric potential is manipulated to control the crystal assembly process, which is directly tunable from its voltage and frequency dependence (Fig. 10C and D). A simple proportional control law

$$[V, \omega] = \begin{cases} [-K\Delta\langle C_6\rangle, 0.1\,\text{MHz}]; & \Delta\langle C_6\rangle < -0.25 \\ [K\Delta\langle C_6\rangle, 1\,\text{MHz}]; & \Delta\langle C_6\rangle \geq -0.25 \end{cases} \quad (8)$$

was used to compute the system inputs [5], where V denotes voltage, ω denotes frequency, K = 4 V denotes the proportional gain, and $\Delta\langle C_6\rangle = \langle C_6\rangle_{\text{SP}} - \langle C_6\rangle_{\text{PV}}$ where SP denotes setpoint and PV denotes process value (i.e., measurement). The variable $\langle C_6\rangle$ is an *order parameter* [5] used to quantify the degree of crystallinity for any configuration of colloidal particles. Specifically, $\langle C_6\rangle$ denotes the number of hexagonal close-packed (hcp) neighbors around each particle averaged over all particles in a given configuration. The results from applying the feedback law (8) to the system in Fig. 10A are shown in Fig. 11, which demonstrates the controlled assembly and disassembly of a colloidal crystal. The use of feedback allows defects in the crystal to be repaired through partial disassembly, repair, and then re-assembly.

The use of order parameters in the latter example enables collapsing the massive amount of information in the measurement of these systems (position of all particles) to a single variable, which simplifies the control strategy at the cost of losing information about the current system state. However, this control strategy may not always be effective, depending on the type of system and order parameter selected. For example, as noted by [5], $\langle C_6\rangle$-like order parameters may not be useful for condensation processes that terminate in amorphous states because they only take on finite values once geometric ordering occurs.

Advanced model-based control approaches can be implemented in a closed-loop fashion using available real-time measurements to optimize the process of self-assembly. An example of such control has been demonstrated in [59] where model predictive control was used to drive the self-assembly of the quadrapole system in Fig. 10A instead of the proportional control strategy in (8). The simulation results indicate that the computed input trajectory is able to accelerate crystallization of the colloidal particles. However, this acceleration is achieved at the price of the computational cost of optimizing over the Langevin-based model. This example demonstrates that the tradeoff between controller complexity and performance can be an important issue in the context of controlling micro- and nano-scale self-assembly.

4. Outlook for future research

The assembly of a large number of small particles into complex ordered structures can aid in the bottom-up engineering of devices with novel characteristics. The primary challenges in the control of micro- and nano-scale self-organizing systems are high-dimensional stochastic dynamics, lack of sensing, limited actuation,

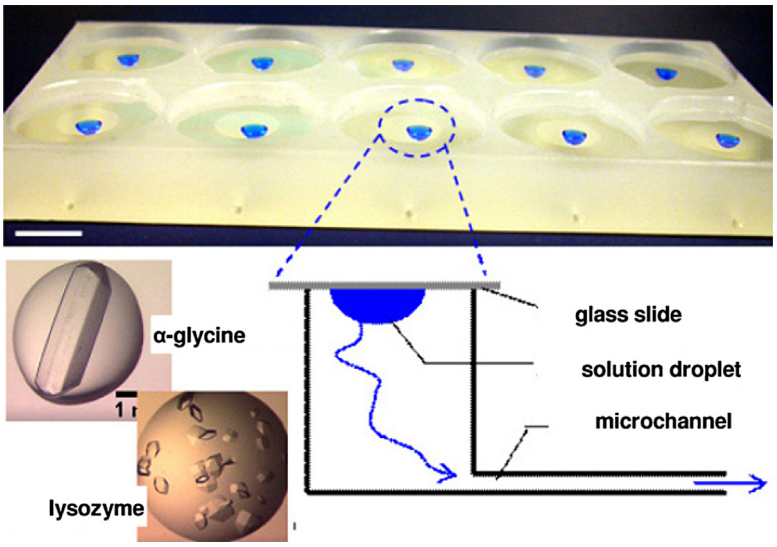

Fig. 8. Image of a microfluidic platform that uses evaporation to induce nucleation in microliter droplets (see [18,19]). The evaporation rate in each droplet is specified by the partial pressure of water at the droplet surface, the area and length of the channel that connects the droplet to external air, and the humidity of the external air. This apparatus can be used for open- or closed-loop control based on manipulation of the evaporation rate. Reprinted from [17] with permission from Elsevier.

and the formation of kinetically trapped configurations. This article provides an overview of the recent developments in active self-assembly and open- and closed-loop control of small-scale self-assembly systems.

A promising research direction is the design of particles that enables active control of particle interactions and increases particle specificity toward forming a desired structure. The design of particles for active self-assembly induces what can be interpreted as *internal feedback* where each particle responds to its local environment by exchanging information between different components of the system. Internal feedback allows the particles to reach a consensus about the desired structure of the self-organizing system based on the state of all particles. Such an approach offers vast opportunities for sensing and actuation at the micro- and nano-scale.

Actuators can be introduced either globally (changes felt throughout the system) or locally (changes felt only in a local environment) to drive the system toward the desired ordered structure. Simple open-loop control policies have been developed to facilitate self-assembly for a variety of systems by manipulating global fields of variables such as temperature [7] and pH [56]. Examples of these strategies were discussed in detail in Section 3.2. A major drawback of these open-loop strategies is their lack of robustness such that small perturbations during the self-assembly process can lead to undesired structures (e.g., kinetically trapped states). Recent work on the self-assembly of the protein clathrin suggests that these open-loop strategies can be made more robust by replacing strong specific interactions between particles with multiple weak specific interactions [56]. These weak interactions allow the system to escape kinetically trapped states during the assembly process while still forming the desired self-assembled structure.

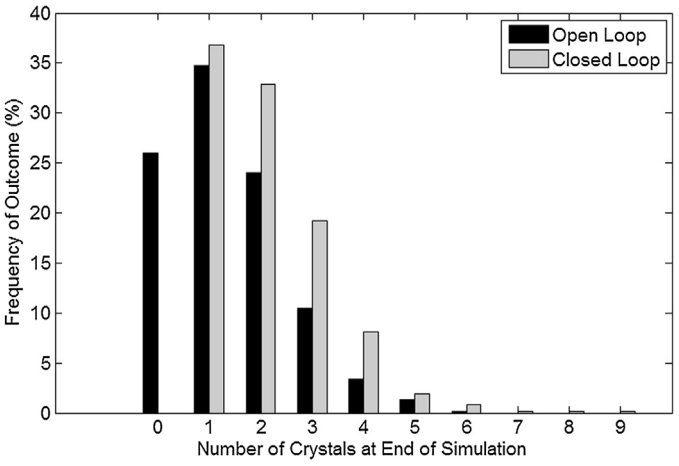

Fig. 9. Comparison of closed-loop (feedback) and open-loop control policies for microliter droplet crystallization for the system in Fig. 8. The output is the number of crystals at the final time in the simulation while the manipulated variable (input) is the volume of the droplet. A proportional controller was used to incorporate feedback with the desired number of crystals (i.e., setpoint) set to 1. The open-loop input trajectory was taken to be the average of the input trajectories for the 1000 closed-loop simulations. Other intuitive open-loop input trajectories (e.g., those corresponding to fastest/slowest induction time in the 1000 simulations) resulted in even worse performance.

An alternative method to create more robust open-loop control policies is to introduce local actuation at the micro- and nano-scale. Local manipulation of fields (e.g., temperature, concentration, pH, electric field, and magnetic field) has been shown in simulations to drive the system toward a particular desired configuration with a high probability [52,53,55]. Methods for qualitative and quantitative shaping of the energy landscape through manipulation of these fields were reviewed in Section 3.2.

Currently, it is common to apply only one or two of these approaches at a time. However, integrating global and local actuators with "optimally-designed" particles could enable precise control of extremely complex structures during the self-assembly process. We believe this is a key direction for future research in controlled self-assembly.

Another promising research direction is the use of model-based control to optimize the self-assembly process through manipulation of local and/or global system inputs. In particular, model predictive control can handle complex multivariate dynamics and competing sets of objectives while satisfying system constraints. The control performance largely depends on the quality of the system model, which indicates that the development of compact models for complex system dynamics in self-assembly is a key need. As discussed throughout this article, common models for these systems include the Langevin equation, the Master equation, and partition functions, whose dimensionality/complexity limit their applicability for many systems of practical importance.

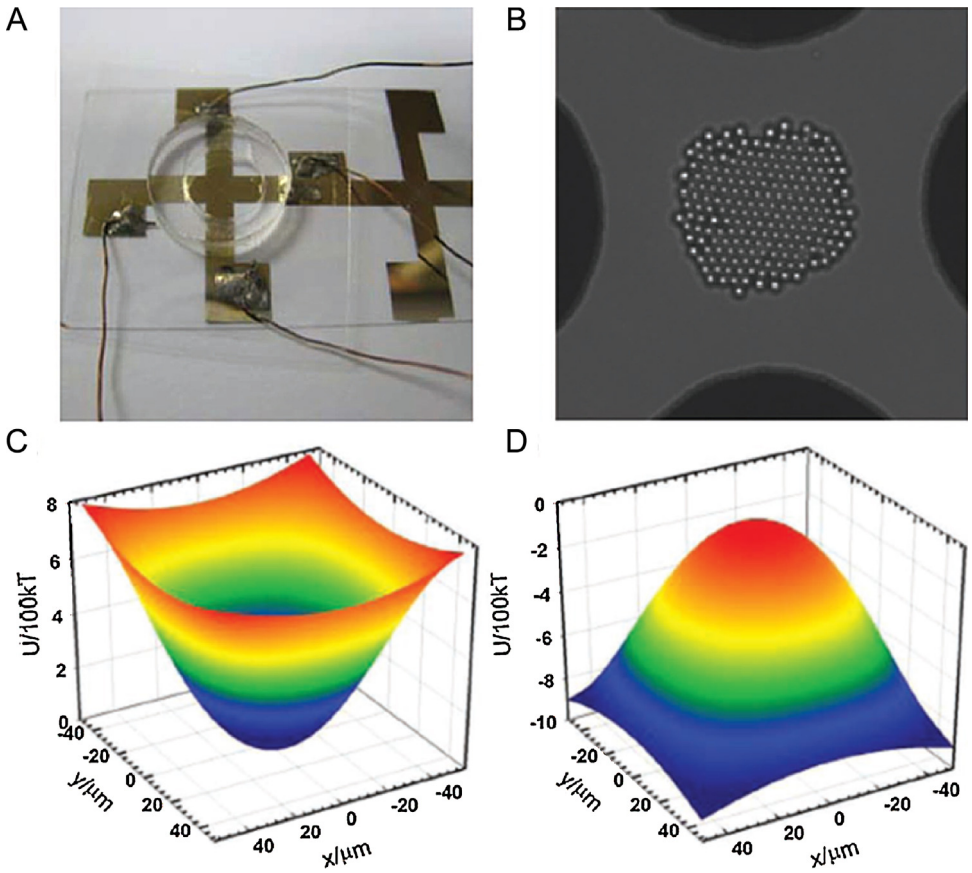

Fig. 10. Experimental apparatus used for closed-loop control of colloidal assembly. (A) Experimental setup of gold film quadrupole electrodes on a glass slide microscope slide and an o-ring container that houses an aqueous dispersion of silica colloidal particles. (B) Example image taken using optical microscopy used as a sensor for system measurements. Theoretical Cartesian coordinate-based potential energy wells were computed, using the electrode center as a reference, at (C) $V = 4$ V, $\omega = 1$ MHz and (D) $V = 4$ V, $\omega = 0.1$ MHz. Reprinted (adapted) from [5] with permission from John Wiley and Sons.

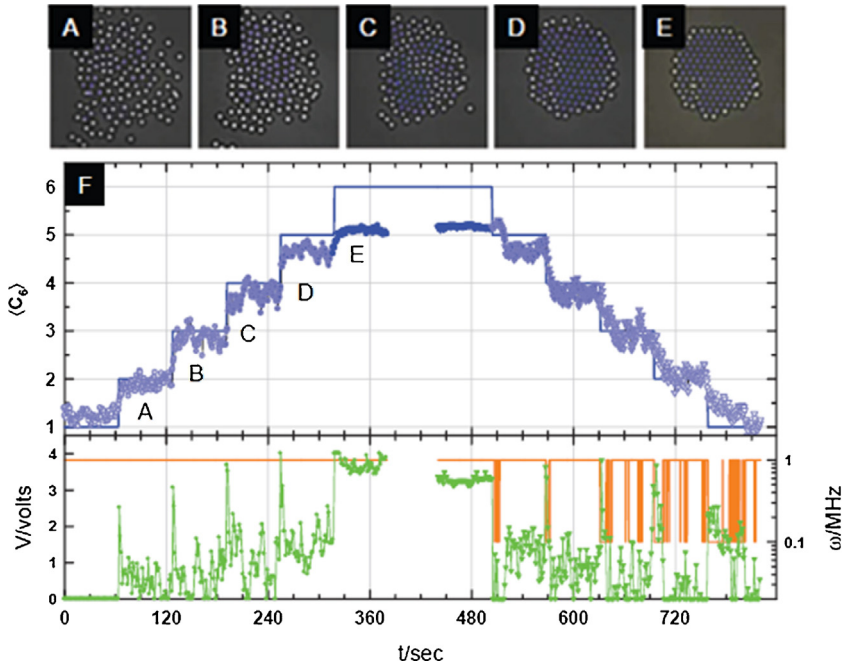

Fig. 11. Feedback controlled self-assembly of a colloidal crystal containing 130 particles using the control law in (8). Optical microscopy measurements with $\langle C_6 \rangle_{SP}$ equal to (A) 2, (B) 3, (C) 4, (D) 5, And (E) 6. (F) Feedback-controlled self-assembly (0–360 s) and disassembly (480–720 s). The top pane shows $\langle C_6 \rangle_{SP}$ (solid blue line) and $\langle C_6 \rangle_{PV}$ (blue points) versus time. The bottom pane shows the manipulated variables voltage V (green line) and frequency ω (orange line) versus time computed using (8). Reprinted (adapted) from [5] with permission from John Wiley and Sons. (For interpretation of the references to color in this figure legend, the reader is referred to the web version of this article.)

The use of feedback (measurements) in the control policy is another way to make the system more robust to stochasticity and disturbances by counteracting this uncertainty with available measurements from real-time sensors. These closed-loop approaches require the development of advanced sensing technologies to monitor local system properties (e.g., positions of all particles). Real-time estimation of the system state is required when implementing most advanced model-based control strategies. A key challenge in this space is being able to utilize the system measurement within a complex model of the self-assembly process in real-time. One alternative, discussed in Section 3.3, is the use of order parameters to collapse the large amount of detailed information within the measurement to a relatively small number of variables. In addition, models in terms of these order parameters (see e.g., [59]) can be much cheaper to evaluate than their full-information counterparts. Another alternative is to employ advanced control strategies whose online computations are based purely on input-output models used in concert with output estimation. Control algorithms that employ this approach for systems with stochastic uncertainties [34] may be promising for application to self-assembly.

The development and use of nano-scale sensors for control of micro- and nano-scale self-assembly is an important route to explore. Some recent examples of nano-scale sensors include: (1) single-walled carbon nanotubes (SWCNTs), which exhibit discrete changes in the fluorescence signal when molecules adsorb and desorb from the SWCNT surface [60], (2) asymmetric catalytic particles that use chemical reactions for self-propulsion so that the speed of the catalyst is indicative of the local concentration [61], and (3) gold nanoshells with a pH-sensitive adsorbate that can be used as a standalone all-optical nano-scale pH meter [62]. Experimental verification of advanced control methods utilizing these types of nano-scale sensors remains largely unexplored in the area of controlled self-assembly.

Acknowledgments

Financial support is acknowledged from the U.S. National Science Foundation Graduate Research Fellowship and the Edwin R. Gilliland Professorship at the Massachusetts Institute of Technology.

References

[1] G.M. Whitesides, B. Grzybowski, Self-assembly at all scales, Science 295 (5564) (2002) 2418–2421.
[2] G.M. Whitesides, M. Boncheva, Beyond molecules: self-assembly of mesoscopic and macroscopic components, Proc. Natl. Acad. Sci. 99 (8) (2002) 4769–4774.
[3] S.C. Glotzer, J.A. Anderson, Nanoparticle assembly: made to order, Nat. Mater. 9 (11) (2010) 885–887.
[4] M.R. Jones, C.A. Mirkin, Materials science: self-assembly gets new direction, Nature 491 (7422) (2012) 42–43.
[5] J.J. Juárez, M.A. Bevan, Feedback controlled colloidal self-assembly, Adv. Funct. Mater. 22 (18) (2012) 3833–3839.
[6] S. Srivastava, A. Santos, K. Critchley, K.-S. Kim, P. Podsiadlo, K. Sun, J. Lee, C. Xu, G.D. Lilly, S.C. Glotzer, N.A. Kotov, Light-controlled self-assembly of semiconductor nanoparticles into twisted ribbons, Science 327 (5971) (2010) 1355–1359.
[7] J.W. Swan, J.L. Bauer, Y. Liu, E.M. Furst, Directed colloidal self-assembly in toggled magnetic fields, Soft Matter 10 (8) (2014) 1102–1109.
[8] Q. Chen, S.C. Bae, S. Granick, Directed self-assembly of a colloidal kagome lattice, Nature 469 (7330) (2011) 381–384.
[9] M. Grzelczak, J. Vermant, E.M. Furst, L.M. Liz-Marzán, Directed self-assembly of nanoparticles, ACS Nano 4 (7) (2010) 3591–3605.
[10] Q. Li, J.A. Lewis, Nanoparticle inks for directed assembly of three-dimensional periodic structures, Adv. Mater. 15 (19) (2003) 1639–1643.
[11] M.J. Cima, L.G. Cima, Tissue regeneration matrices by solid free form fabrication techniques, US Patent 5,518,680 (May 21 1996).
[12] G. Mapili, Y. Lu, S. Chen, K. Roy, Laser-layered microfabrication of spatially patterned functionalized tissue-engineering scaffolds, J. Biomed. Mater. Res. Part B: Appl. Biomater. 75 (2) (2005) 414–424.
[13] X. Liu, Y. Zhang, D.K. Goswami, J.S. Okasinski, K. Salaita, P. Sun, M.J. Bedzyk, C.A. Mirkin, The controlled evolution of a polymer single crystal, Science 307 (5716) (2005) 1763–1766.
[14] S. Kufer, E. Puchner, H. Gumpp, T. Liedl, H. Gaub, Single-molecule cut-and-paste surface assembly, Science 319 (5863) (2008) 594–596.
[15] J. Moon, A.C. Caballero, L. Hozer, Y.-M. Chiang, M.J. Cima, Fabrication of functionally graded reaction infiltrated SiC-Si composite by three-dimensional printing 3DP™ process, Mater. Sci. Eng. A 298 (1) (2001) 110–119.
[16] J.V. Beck, K.J. Arnold, Parameter Estimation in Engineering and Science, John Wiley & Sons, New York, 1977.
[17] Z.W. Ulissi, M.S. Strano, R.D. Braatz, Control of nano and microchemical systems, Comput. Chem. Eng. 51 (2013) 149–156.
[18] S. Talreja, P.J. Kenis, C.F. Zukoski, A kinetic model to simulate protein crystal growth in an evaporation-based crystallization platform, Langmuir 23 (8) (2007) 4516–4522.
[19] S. Talreja, S.L. Perry, S. Guha, V. Bhamidi, C.F. Zukoski, P.J. Kenis, Determination of the phase diagram for soluble and membrane proteins, J. Phys. Chem. B 114 (13) (2010) 4432–4441.
[20] D.S. Lemons, A. Gythiel, Paul Langevins 1908 paper on the theory of Brownian motion [sur la théorie du mouvement brownien, cr acad. sci. (paris) 146, 530–533 (1908)], Am. J. Phys. 65 (11) (1997) 1079–1081.
[21] W. Coffey, Y.P. Kalmykov, J.T. Waldron, The Langevin Equation: With Applications to Stochastic Problems in Physics, Chemistry, and Electrical Engineering, 2nd edition, World Scientific, Singapore, 2004.
[22] R. Zwanzig, Nonlinear generalized Langevin equations, J. Stat. Phys. 9 (3) (1973) 215–220.
[23] B. Øksendal, Stochastic Differential Equations: An Introduction with Applications, Springer, Heidelberg, New York, Dordrecht, London, 2003.
[24] M.F. Hagan, Modeling Viral Capsid Assembly, vol. 155, John Wiley & Sons, Inc, Hoboken, NJ, 2014.
[25] S. Pankavich, Z. Shreif, Y. Miao, P. Ortoleva, Self-assembly of nanocomponents into composite structures: derivation and simulation of Langevin equations, J. Chem. Phys. 130 (19) (2009) 194115.
[26] K.A. Fichthorn, W.H. Weinberg, Theoretical foundations of dynamical Monte Carlo simulations, J. Chem. Phys. 95 (2) (1991) 1090–1096.
[27] D.G. Kendall, Stochastic processes and population growth-symposium on stochastic processes, J. R. Stat. Soc. Ser. B 11 (2) (1949) 230–264.
[28] I.G. Kevrekidis, C.W. Gear, J.M. Hyman, P.G. Kevrekidis, O. Runborg, C. Theodoropoulos, Equation-free, coarse-grained multiscale computation: enabling macroscopic simulators to perform system-level analysis, Commun. Math. Sci. 1 (4) (2003) 715–762.
[29] I.G. Kevrekidis, C.W. Gear, G. Hummer, Equation-free: the computer-aided analysis of complex multiscale systems, AIChE J. 50 (7) (2004) 1346–1355.
[30] H.-A. Klok, S. Lecommandoux, Supramolecular materials via block copolymer self-assembly, Adv. Mater. 13 (16) (2001) 1217–1229.
[31] L. Goh, K. Chen, V. Bhamidi, G. He, N.C. Kee, P.J. Kenis, C.F. Zukoski III, R.D. Braatz, A stochastic model for nucleation kinetics determination in droplet-based microfluidic systems, Crystal Growth Des. 10 (6) (2010) 2515–2521.
[32] Q. Chen, J.K. Whitmer, S. Jiang, S.C. Bae, E. Luijten, S. Granick, Supracolloidal reaction kinetics of janus spheres, Science 331 (6014) (2011) 199–202.
[33] M.W. Hermanto, M.-S. Chiu, X.-Y. Woo, R.D. Braatz, Robust optimal control of polymorphic transformation in batch crystallization, AIChE J. 53 (10) (2007) 2643–2650.
[34] A. Mesbah, S. Streif, R. Findeisen, R.D. Braatz, Stochastic nonlinear model predictive control with probabilistic constraints, in: Proc. of the American Control Conference, Portland, OR, 2014, pp. 2413–2419.
[35] K.G. Libbrecht, The physics of snow crystals, Rep. Prog. Phys. 68 (4) (2005) 855.
[36] S.C. Glotzer, M.J. Solomon, Anisotropy of building blocks and their assembly into complex structures, Nat. Mater. 6 (8) (2007) 557–562.
[37] P.F. Damasceno, M. Engel, S.C. Glotzer, Predictive self-assembly of polyhedra into complex structures, Science 337 (6093) (2012) 453–457.
[38] J. Haleblian, W. McCrone, Pharmaceutical applications of polymorphism, J. Pharm. Sci. 58 (8) (1969) 911–929.
[39] R. Braatz, R. Alkire, E. Seebauer, E. Rusli, R. Gunawan, T. Drews, X. Li, Y. He, Perspectives on the design and control of multiscale systems, J. Process Contr. 16 (3) (2006) 193–204.
[40] R.D. Braatz, R.C. Alkire, E.G. Seebauer, T.O. Drews, E. Rusli, M. Karulkar, F. Xue, Y. Qin, M.Y. Jung, R. Gunawan, A multiscale systems approach to microelectronic processes, Comput. Chem. Eng. 30 (10) (2006) 1643–1656.
[41] E. Klavins, Programmable self-assembly, IEEE Contr. Syst. Mag. 27 (4) (2007) 43–56.
[42] Y. Xue, M.A. Grover, Optimal design for active self-assembly system, in: Proceedings of the American Control Conference, San Francisco, CA, 2011, pp. 3269–3274.
[43] D. Arbuckle, A.A. Requicha, Active self-assembly, in: Proceedings of the IEEE International Conference on Robotics and Automation, New Orleans, LA, 2004, pp. 896–901.
[44] S. Glotzer, M. Solomon, N.A. Kotov, Self assembly: from nanoscale to microscale colloids, AIChE J. 50 (12) (2004) 2978–2985.
[45] E. Edlund, O. Lindgren, M.N. Jacobi, Predicting self-assembled patterns on spheres with multicomponent coatings, Soft Matter 10 (17) (2014) 2955–2960.
[46] Y. Wang, Y. Wang, D.R. Breed, V.N. Manoharan, L. Feng, A.D. Hollingsworth, M. Weck, D.J. Pine, Colloids with valence and specific directional bonding, Nature 491 (7422) (2012) 51–55.

[47] O. Idan, A. Lam, J. Kamcev, J. Gonzales, A. Agarwal, H. Hess, Nanoscale transport enables active self-assembly of millimeter-scale wires, Nano Lett. 12 (1) (2011) 240–245.
[48] S. Granick, S. Jiang, Q. Chen, Janus particles, Phys. Today 62 (2009) 68–69.
[49] L. Hong, A. Cacciuto, E. Luijten, S. Granick, Clusters of amphiphilic colloidal spheres, Langmuir 24 (3) (2008) 621–625.
[50] M.R.A. Bakar, Z.K. Nagy, C.D. Rielly, Seeded batch cooling crystallization with temperature cycling for the control of size uniformity and polymorphic purity of sulfathiazole crystals, Org. Process Res. Dev. 13 (6) (2009) 1343–1356.
[51] M. Jiang, X. Zhu, M.C. Molaro, M.L. Rasche, H. Zhang, K. Chadwick, D.M. Raimondo, K.-K.K. Kim, L. Zhou, Z. Zhu, M.H. Wong, D. O'Grady, D. Hebrault, J. Tedesco, R.D. Braatz, Modification of crystal shape through deep temperature cycling, Ind. Eng. Chem. Res. 53 (13) (2014) 5325–5336.
[52] E.O.P. Solis, P.I. Barton, G. Stephanopoulos, Controlled formation of nanostructures with desired geometries. 1. Robust static structures, Ind. Eng. Chem. Res. 49 (17) (2010) 7728–7745.
[53] E.O.P. Solis, P.I. Barton, G. Stephanopoulos, Controlled formation of nanostructures with desired geometries. 2. Robust dynamic paths, Ind. Eng. Chem. Res. 49 (17) (2010) 7746–7757.
[54] C.-A. Palma, M. Cecchini, P. Samorì, Predicting self-assembly: from empirism to determinism, Chem. Soc. Rev. 41 (10) (2012) 3713–3730.
[55] R. Lakerveld, G. Stephanopoulos, P.I. Barton, A master-equation approach to simulate kinetic traps during directed self-assembly, J. Chem. Phys. 136 (18) (2012) 184109.
[56] A.P. Schoen, N. Cordella, S. Mehraeen, M.A. Arunagirinathan, A.J. Spakowitz, S.C. Heilshorn, Dynamic remodelling of disordered protein aggregates is an alternative pathway to achieve robust self-assembly of nanostructures, Soft Matter 9 (38) (2013) 9137–9145.
[57] D.E. Wakeham, C.-Y. Chen, B. Greene, P.K. Hwang, F.M. Brodsky, Clathrin self-assembly involves coordinated weak interactions favorable for cellular regulation, EMBO J. 22 (19) (2003) 4980–4990.
[58] S. Whitelam, Control of pathways and yields of protein crystallization through the interplay of nonspecific and specific attractions, Phys. Rev. Lett. 105 (8) (2010) 088102.
[59] X. Tang, Y. Xue, M.A. Grover, Colloidal self-assembly with model predictive control, in: Proceedings of the American Control Conference, Washington, DC, 2013, pp. 4228–4233.
[60] L. Cognet, D.A. Tsyboulski, J.-D.R. Rocha, C.D. Doyle, J.M. Tour, R.B. Weisman, Stepwise quenching of exciton fluorescence in carbon nanotubes by single-molecule reactions, Science 316 (5830) (2007) 1465–1468.
[61] D. Kagan, P. Calvo-Marzal, S. Balasubramanian, S. Sattayasamitsathit, K.M. Manesh, G.-U. Flechsig, J. Wang, Chemical sensing based on catalytic nanomotors: motion-based detection of trace silver, J. Am. Chem. Soc. 131 (34) (2009) 12082–12083.
[62] S.W. Bishnoi, C.J. Rozell, C.S. Levin, M.K. Gheith, B.R. Johnson, D.H. Johnson, N.J. Halas, All-optical nanoscale pH meter, Nano Lett. 6 (8) (2006) 1687–1692.